



Research Article

# Polyphenol Enriched Extract of Pomegranate Peel; A Novel Precursor for the Biosynthesis of Zinc Oxide Nanoparticles and Application in Sunscreens

Maryam Kokabi<sup>1,2</sup> , Samad Nejad Ebrahimi<sup>1</sup>

<sup>1</sup>Department of Phytochemistry, Medicinal Plants and Drugs Research Institute, Shahid Beheshti University, Evin, Tehran, Iran.

<sup>2</sup>Department of Marine Biology, Faculty of Marine Science and Technology, University of Hormozgan, Bandar Abbas, Iran.

## Article Info

### Article History:

Received: 29 May 2020

Accepted: 9 July 2020

ePublished: 10 October 2020

### Keywords:

- Green synthesis
- Metal oxide
- Nanotechnology
- Pomegranate
- SPF

## Abstract

**Background:** Green synthesized nanoparticles (NPs) from agricultural wastes is an area of great interest due to it is eco-friendly and profitable. Zinc oxide is an inorganic UV-filter commonly used as UV-blocker in a different industry.

**Methods:** Zinc oxide nanoparticles (ZnO NPs) were successfully biosynthesized using  $Zn(NO_3)_2$  as a substrate by polyphenol enriched fraction (PEF) of pomegranate peel. The biological activity of ZnO NPs was evaluated using MBC and MIC tests for antibacterial and DPPH assay for antioxidant potential. Sunscreen potential of NPs was determined after applying them in water-in-oil emulsions.

**Results:** UV-Vis and FT-IR spectroscopy techniques confirmed the formation of ZnO NPs. FE-SEM characterized the morphology and purity of the biosynthesized NPs with EDAX and XRD data. The average crystalline size of ZnO NPs was found to be 22 nm. FT-IR spectroscopy revealed the role of phenolic compounds in the formation and stability of ZnO NPs. The antibacterial activity of PEF and its biosynthesized ZnO was evaluated against *Staphylococcus aureus* and *Escherichia coli*. The prepared NPs showed a higher antibacterial effect than the commercial ZnO NPs. Interestingly, the antioxidant activity was also detected for obtained NPs. The PEF powder also exhibited higher antibacterial and antioxidant activity than the standards. Furthermore, the *in vitro* sun protection factors were estimated after applying NPs in water-in-oil emulsions.

**Conclusion:** This study highlighted the possibility of using PEF of pomegranate peel for the biosynthesis of ZnO NPs as well as applying its NPs in sunscreens to achieve a safe alternative to harmful chemical UV-filters commonly used in cosmetics.

## Introduction

Today, many chemicals are applied in sunscreen formulations as UV-absorber that cause side effects and release into the natural ecosystems.<sup>1</sup> There are two types of ultraviolet filters: organic and inorganic. Zinc oxide is an inorganic UV-filters commonly used in personal care products for different functions such as skin protection and UV-blocker. Commercially UV-filters are mostly chemically synthesized using some toxic reagents.<sup>2</sup> The growing concerns on environmental pollution have encouraged the development of a biological approach for the synthesis of nanoparticles (NPs). In this regard, green techniques for the synthesis of physical UV-filters such as  $TiO_2$  and ZnO has attracted considerable interest. Mainly due to the worldwide tendency to use natural-based personal care products.<sup>3</sup>

Using the agricultural by-products as a precursor for

green synthesis has advantageous in several ways. Many studies have been reported biosynthesis of metal oxide NPs using natural substances such as fruits,<sup>4</sup> plants,<sup>5-6</sup> microorganisms,<sup>7</sup> or biowaste.<sup>8</sup> However, in the technical scope, using bio-waste is more beneficial due to features like availability, eco-friendly and cost-effectiveness.

*Punica granatum* L., commonly known as pomegranate, is an important agricultural crop widely cultivated in Iran and some other countries such as India, China, Japan, Turkey, and the United States. Pomegranate peel is the non-edible portion of this fruit, which makes up about 40-50% of its whole weight and considered as a waste of industrial products such as pomegranate juice and sauce.<sup>9</sup> The literature survey shows the presence of a considerable amount of bioactive compounds in pomegranates peels such as ellagitannins, phenolic acids, polyphenols and

\*Corresponding Author: Samad N. Ebrahimi, E-mail: s\_ebrahimi@sbu.ac.ir

©2021 The Author(s). This is an open access article and applies the Creative Commons Attribution License (<http://creativecommons.org/licenses/by-nc/4.0/>), which permits unrestricted use, distribution, and reproduction in any medium, as long as the original authors and source are cited.

flavonoids in this by-product that can be exploited for different purposes.<sup>10-11</sup>

Here, the polyphenol enriched fraction (PEF) of pomegranate peel was used as a cheap and safe alternative of toxic reagents in the biosynthesis of ZnO NPs. Then, the physical and chemical characterization of the prepared NPs in comparison with its commercial counterpart and the possibility of its application in sunscreens were investigated.

## Materials and Methods

### Chemicals and reference compounds

Methanol and MeCN were obtained from Panreac, Spain. Ethanol from Kimia Alcohol, Zanjan and formic acid, zinc nitrate and Muller Hinton Agar from Merck company. Gallic acid and DPPH were purchased from Sigma–Aldrich Chemicals Co. Commercial ZnO NPs was purchased from Petroplastic Co. The polystyrene adsorption resin (Diaion<sup>®</sup> HP-20), was purchased from Mitsubishi Chemical (Tokyo, Japan). The bacteria strains were obtained from Pasture Institute, Tehran, Iran.

### Preparation of polyphenol enriched fraction

The dried pomegranate peels were powdered using a grinder. The obtained powder (500 g) extracted using ethanol-water (80:20 v/v) by the maceration method for 72 h. The extract evaporated using a rotary evaporator under vacuum at 40°C to obtain dry gummy residue (120 g). Aliquot of peels extract (50 g) suspended in deionized water and homogenized by sonication. The obtained liquid loaded on the Diaion<sup>®</sup> HP-20 resin column (Mitsubishi Chemical, Tokyo, Japan) (70 cm × 8 cm) and washed with water (5.0 L) and ethanol (5.0 L). The ethanol fraction evaporated by rotary evaporator and freeze-dried (22.1 g) called a polyphenolic enriched fraction (PEF). The obtained powder stored in the refrigerator for the next step and analyses with HPLC. The extract was analyzed with waters liquid chromatography equipment consisting of a 2695 Separations Module (USA), an autosampler equipped with a 100 µl loop and Photodiode Array Detectors (PDA) using a RP-C18 column. The solvent system used a mixture of MeCN+0.1% formic acid (A) and H<sub>2</sub>O+0.1% formic acid (B), the following gradient was applied: 2% (A) in 20 min; 2% to 10% (A) in 5 min; 10% to 20% (A) in 20 min; 20% to 100% (A) in 15 min; 100% (A) in 10 min; all process take time about 66 min, the flow rate was 0.4 ml/min and the injection volume was 20 µl. The UV absorbance was measured at 254 nm.

### Synthesis of ZnO NPs

The amount of 85 mg of the PEF powder was completely dissolved in 10 ml deionized water and dispersed into the 190 ml solution of 0.2 M zinc nitrate under continuous stirring at 60°C for 2 h to complete the reaction. Then the pH of the reaction solution was adjusted on 6 when a precipitate appeared in the vessel. The yellow-colored precipitate was collected by centrifugation at 6000 rpm

for 15 min and washed thoroughly with deionized water. The product was dried at 80°C followed by calcination at 400°C for 2 h to completely converted Zn(OH)<sub>2</sub> into ZnO NPs.<sup>4</sup> Finally, an opaque white pelt was obtained and ground to produce fine ZnO powder. The prepared ZnO nanopowder called PEF-ZnONPs and was used for further characterization for their optical and nanostructural properties.

### Characterization of zinc oxide NPs

The optical absorption spectrum of ZnO nanopowder was obtained using a UV-Vis spectrophotometer (Shimadzu, UV-2501PC) in the range of 200 to 700 nm. Fourier transform infrared (FT-IR) spectra were established for the analysis of functional groups using an FT-IR spectrometer (Tensor 27, Bruker). The prepared ZnO NPs were homogenized with KBr in a ratio of 1:100 and pellets were prepared for the FT-IR measurements. The IR spectra of PEF powder and commercial ZnO NPs (US-NANO) were also analyzed with the same method. The purity and grain size of the dried powder of ZnO NPs was evaluated by the X-ray diffraction (XRD) method operating with Cu K $\alpha$  radiation in wavelength  $\lambda = 0.15406$  nm over the scan range of  $2\theta = 1-80^\circ$ . Morphology of the PEF-ZnO NPs, along with the elemental analysis (EDXA), was demonstrated via Field Emission Scanning Electron Microscopy (FE-SEM) (MIRA3 TESCAN).

The average crystalline size of the biosynthesized ZnO NPs was calculated by using The Debye Scherrer's formula as follows:

$$D = \frac{k\lambda}{\beta \cos \theta} \quad \text{Eq. (1)}$$

In which D is the mean crystallite size, K is the Scherrer constant equal to 0.93,  $\lambda$  is the X-ray wavelength was used (1.5406 Å),  $\beta$  the full width at half- maximum (FWHM) of the considered peak and  $\theta$  is the Bragg angle.<sup>12</sup>

### Antibacterial evaluation

Antibacterial properties of biosynthesized and commercial NPs, as well as PEF powder, were tested by serial dilution method using two standard strains of Gram-positive (*Staphylococcus aureus*, ATCC 1431) and Gram-negative (*Escherichia coli*, ATCC 1390) bacteria. Suspensions of both ZnO NPs along with PEF powder of pomegranate peel were prepared in deionized water. Afterward, a serial dilution from 0.125 to 32 mg/ml for each sample was prepared in sterile Muller Hinton broth medium using a 96-well plate. After 24 h incubation at 37 °C, the lowest concentration of samples that prevents the growth of the pathogens was recorded as Minimum inhibitory concentration (MIC). Those concentrations with inhibition performance in the MIC test were transferred to fresh nutrient agar media for MBC (minimum bactericidal concentration) screening. All treatments exposed for 24 h at 37 °C. The lowest concentration of samples from which the bacteria do not

grow on the surface of culture media was considered as MBC value.<sup>13</sup> The results were compared with a commonly used antibiotic Ampicillin.

### Radical scavenging activity

The antioxidant potency of both NPs along with PEF powder of pomegranate peel was evaluated by DPPH assay. Different concentrations (4, 12, 20, 40, 80, 140, and 240 µg/ml) of all samples were prepared in a 96-well microplate and exposed to 40 µg/ml methanolic solution of DPPH (2,2-diphenyl-1-picrylhydrazyl). The same concentration of methanol and DPPH was used as the control without any NPs or extract. Gallic acid was served as a positive control. The reactive solutions were left in the darkness at room temperature for 20 min. Then, the absorbance at 517 nm was taken using a microplate reader (Epoch12, Bio Tek, USA). All of the experiments were performed in triplicate. The percent antioxidant activity of different samples was calculated as follows:<sup>14</sup>

$$\text{DPPH scavenging activity (\%)} = \frac{Ac - As}{Ac} \times 100 \quad \text{Eq. (2)}$$

Where  $A_c$  refers to the absorbance of the control, and  $A_s$  is the absorbance of the sample.

The antioxidant capacity of each sample was estimated in terms of  $IC_{50}$  using a nonlinear regression algorithm.  $IC_{50}$  or Inhibition Concentration is defined as the concentration of an antioxidant required to lead to a 50% inhibition of the DPPH radical absorbance.<sup>15</sup>

### Preparation of emulsion

For preparing the emulsion, 5 ml of almond oil and distilled water heated at 45 °C separately. Then, 1.5 g beeswax was melted and homogenized with the oil phase. Distilled water was gradually added to the oil phase under stirring for approximately 30 min. Different samples were added to the water phase. The resultant emulsions were left at room temperature to solidify. Four water-in-oil emulsions were prepared to contain 5% (w/w) of PEF powder of pomegranate peel or commercial/green synthesized ZnO NPs.

### In vitro SPF assessment

The basic emulsion without ingredients was used as control. The sunscreens photoprotection factor (SPF) was estimated by measuring the spectrophotometric absorbance of a film of each emulsion. An amount of 1.3 mg/cm<sup>2</sup> of samples was manually spread over the surface of a transport tape placed on a quartz slide and left to dry in the dark for 30 min. Then, the absorption spectrum of the samples was determined between 290 and 320 nm with three repetitions using Shimadzu UV-2501PC spectrophotometer.<sup>16-17</sup> Then, SPF values were calculated according to the following equation:

$$\text{SPF} = CF \times \sum_{290}^{320} EE(\lambda) \times I(\lambda) \times abs(\lambda) \quad \text{Eq. (3)}$$

In which, CF is the correction factor (=10),  $EE(\lambda)$ , the erythemal effect of spectrum;  $I(\lambda)$  the intensity of solar spectral irradiance;  $abs(\lambda)$  is the absorbance of samples.<sup>18</sup> UV-A protection of emulsions was determined by calculating the ratio of mean UVA1 (340-400 nm) values to total UV (290-400 nm) absorbance curve of samples according to the FDA method described by Wang *et al.*<sup>19</sup> Briefly, the ratio close to one (>0.95) is considered as the highest UV-A protection.

### Statistical analysis

The results are calculated as the average  $\pm$  SD of three replicates (Average  $\pm$ SD; n = 3). One-way analysis of variance (ANOVA) was carried out to determine the significant differences among treatments followed by Student-Newman-Keuls (S-N-K) posthoc test at 95% confidence ( $P < 0.05$ ) using SPSS software (SPSS 22).  $IC_{50}$  values were calculated using the slope equations of the dose-response curves ( $Y = a + bX$ ).

## Results and Discussion

### Spectrophotometry

The application HP-20 Diaion resin for treatment of hydroalcoholic extract of pomegranate peel allowed obtaining polyphenol enriched fraction (PEF).<sup>20-21</sup> The HPLC-UV analysis of PEF represented in Figure 1. The reaction progress of PEF with the zinc nitrate solution was monitored using a UV-Vis spectrophotometer. The optical absorption spectra of the reaction mixture were recorded at a concentration interval of 1, 20, 30, 40, and 50 ml of PEF solution. Figure 2a depicted the rapid biosynthesis of ZnO NPs immediately after adding more PEF solution. This can be attributed to the rapid and more production of ZnO NPs. All the spectra showed two absorption maxima on the spectrum in 257 and 320 nm (Figure 2a). These results are in agreement with Talam *et al.*<sup>22</sup> that reported two absorption bands at about 258 and 355 nm on the absorbance spectra of ZnO NPs.

Additionally, the UV-Vis absorption spectrum of obtained PEF-ZnO nanopowder showed a sharp absorbance peak at 370 nm (Figure 2b), which is highly specific for ZnO NPs. Elumalai and Velmurugan (2015), reported the

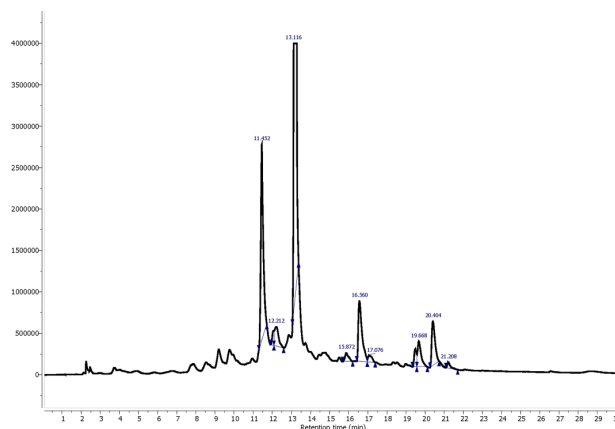
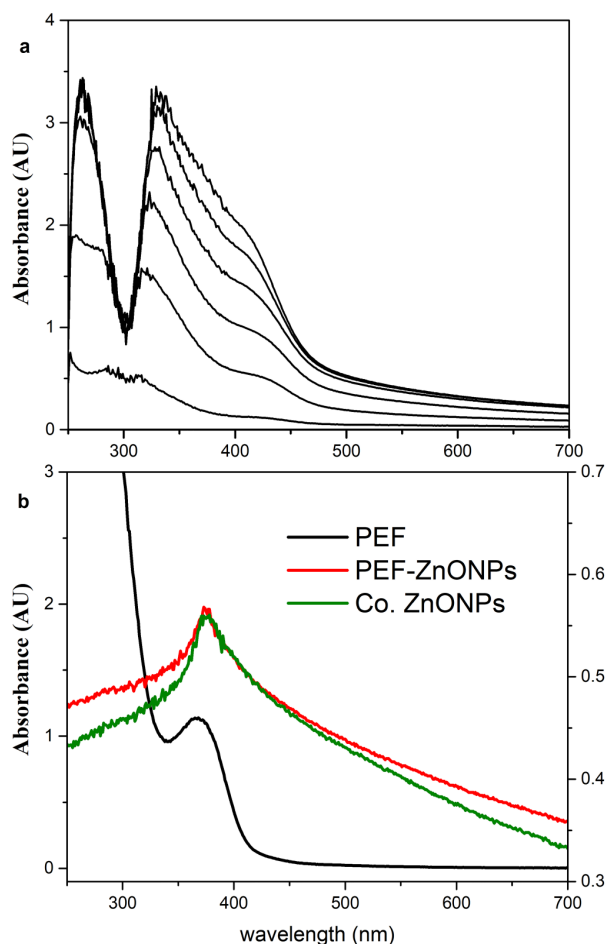


Figure 1. HPLC-UV chromatogram of PEF at 254 nm.



**Figure 2.** (a) UV-VIS spectra of reaction development of PEF of pomegranate peel in the solution of  $Zn(NO_3)_2$ . (b) Comparison of UV-Vis spectrum of PEF of pomegranate peel, PEF-ZnO nanoparticles, and the commercial ZnO nanoparticles.

same absorption peak for the green synthesized ZnO NPs using *Azadirachta indica* (L.).<sup>4</sup> The intense absorption at the wavelength of 370 nm is due to the transitions of electrons from the HOMO to the LUMO molecular orbital level.<sup>23</sup> Aminuzzaman *et al.* and Ali *et al.* also recorded the absorption peak of 370 and 375 nm for their biosynthesized ZnO NPs, respectively.<sup>4,24</sup> The UV-Visible spectra of PEF of pomegranate peel, PEF-ZnO NPs, and the commercial ZnO NPs, in an aqueous suspension were

compared in Figure 2b. The PEF of pomegranate peel showed a maximum wavelength in the UV-A region of 365 nm. According to the literature, phenolic compounds exhibit adsorption in the range of 320–380.<sup>25</sup> The spectra of PEF-ZnO NPs, and the commercial ZnO NPs, revealed the same absorption peak at 370 nm (Figure 2).

#### X-ray diffraction

Figure 3 presented the phase and crystalline structure of biologically synthesized PEF-ZnO NPs detected by X-ray diffraction measurements. The diffraction pattern showed intense peaks at  $2\theta$  values of 31.71, 34.37, 36.21, 47.51, 56.56, 62.81, 67.93, and 69.1 proves the good crystalline nature of NPs and corresponds to (100), (002), (101), (102), (110), (103), (112) and (201) plane, respectively for ZnO (Figure 3). All of the diffraction peaks are confirmed the spherical and hexagonal structure of biosynthesized PEF-ZnO NPs when it was compared with JCPDS card No. 89-7102.<sup>26-27</sup> Besides, the narrow and strong diffraction peaks of the spectrum confirm the crystalline nature as well as the high purity of biologically synthesized PEF-ZnO NPs (Figure 3). The average crystal size of the biosynthesized and the commercial ZnO NPs was further found to be 22 and 17 nm, respectively from their XRD line broadening measurement using Debye-Scherrer formula.

#### FT-IR analysis

FT-IR analysis was carried out to identify the possible functional groups involved in biosynthesized zinc oxide. The FT-IR spectra of PEF of pomegranate peel and biosynthesized PEF-ZnO NPs in the range of 400–4000  $cm^{-1}$  are presented in Figure 4. The broad peak at 3409  $cm^{-1}$  corresponds to the -OH group of absorbed water and phenolic compounds. The main absorption peaks in the PEF of pomegranate peel that shifted in PEF-ZnO NPs spectrum detected between 1000  $cm^{-1}$  and 1730  $cm^{-1}$ . The band at 1725  $cm^{-1}$ , probably related to -OH stretching of carboxyl groups.<sup>28</sup> Likewise, the peak at 1611  $cm^{-1}$  can be due to the presence of C=C stretching vibration of aromatic rings<sup>25</sup> and C=O vibrations of amides and carboxylic groups. Moderate absorption peaks in the region of 1449–1500  $cm^{-1}$  could be related to vibration of C-H in  $CH_3$  and  $CH_2$  groups, flavonoids and aromatic rings. The band at

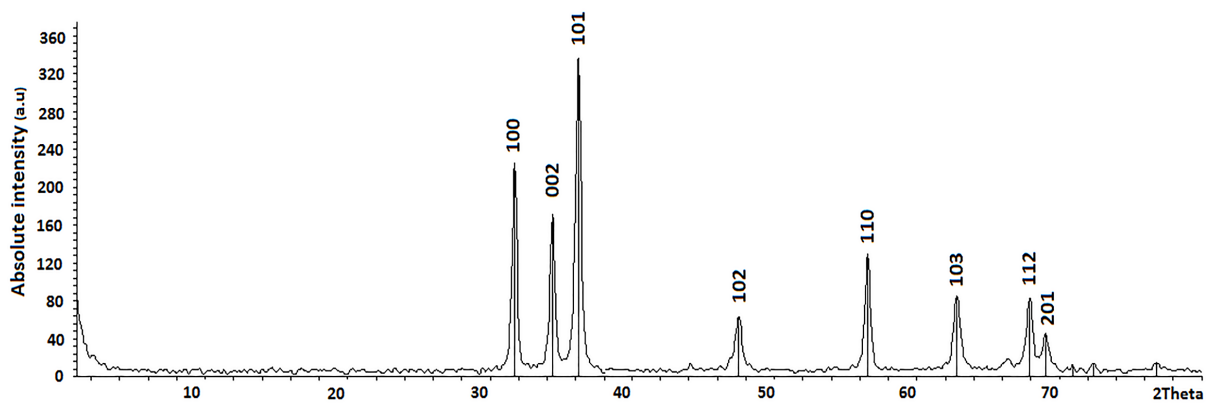


**Figure 3.** XRD pattern of biologically synthesized ZnO NPs using PEF of pomegranate peel.

1321  $\text{cm}^{-1}$  demonstrated the presence of C–O stretching in acid group. The peak at 1178  $\text{cm}^{-1}$  could be attributed to C–O stretching and –OH deformation of primary alcohols. The absorption band at 1036  $\text{cm}^{-1}$  is probably corresponded to primary and secondary alcohols and to C–O group of polyols, such as hydroxyl-flavonoids or to C–O stretching ester group. Weak peaks obtained at 871 and 751  $\text{cm}^{-1}$  could be related to aromatic ring vibration.<sup>29</sup> Phenolic compounds and gallic acid have been reported as major components of pomegranate peel by Singh *et al.*<sup>30</sup> In this study, the FT-IR spectrums indicate that the phenolic groups play an important role in the synthesis process and formation of PEF-ZnO NPs. The presence of a new sharp peak at 438  $\text{cm}^{-1}$  in the FTIR spectrum ascribing the formation of the zinc-oxygen bond of PEF-ZnO NPs (Figure 4a). Generally, the peak in the range of 400 to 600  $\text{cm}^{-1}$  is attributed to Zn–O stretching vibrations.<sup>24,31</sup>

### FESEM and EDAX analysis

Field emission scanning electron microscopy (FESEM) in different magnification ranges was performed to visualize the topology and the mean size of ZnO NPs. Figure 5 demonstrated the spherical morphology and agglomeration of commercial ZnO NPs with the average size of 33 nm in comparison with biosynthesized PEF-ZnO NPs with uniform distribution and particle mean size of 31 nm, possibly to reflect less agglomeration in biosynthesized NPs. The agglomeration occurred probably during the process of precipitation and drying. The obtained PEF-ZnO NPs are smaller than the biosynthesized ZnO NPs (40 nm) from the leaf extract of *Azadirachta indica* (L.) reported by Elumalai and Velmurugan.<sup>23</sup> Santhoshkumar *et al.*<sup>32</sup> also reported the average size of 70 nm for their green synthesized ZnO NPs using *Passiflora caerulea* fresh leaf extract.

The morphological properties of shape, size, and crystalline form of NPs relay on various factors such as preparation methods, precursors and organic ligands (usually in the form of surfactants). In the reaction

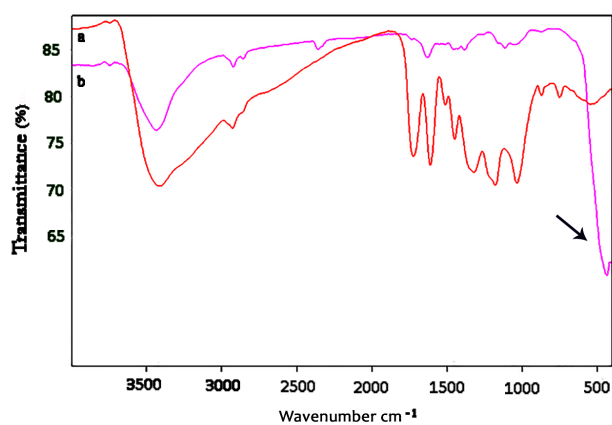


**Figure 4.** FT-IR spectra of (a) PEF of pomegranate peel, and (b) ZnO NPs synthesized from that. The arrow indicates the new sharp peak at 438  $\text{cm}^{-1}$  which is corresponded to zinc-oxygen stretching mode.

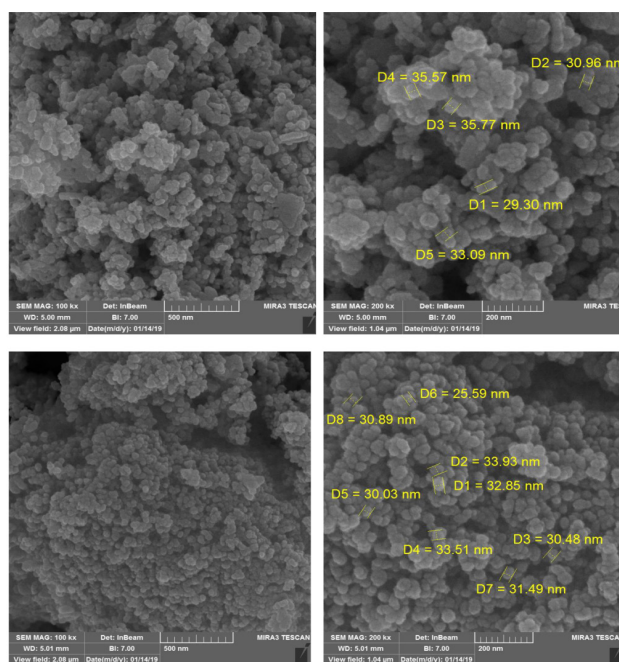


**Figure 5.** FESEM micrographs of commercial ZnO NPs (above) vs. PEF-ZnO nanoparticles (below) in two different magnification.

solution, ligands (surfactant) strongly affect the growth of the NPs. Generally, stronger chelates with metals will result in smaller particles.<sup>33</sup> The plant phytochemicals with antioxidants or reducing power usually play an important role in the synthesise of metal and metal oxide NPs by inducing oxidation and reduction reaction.<sup>32</sup> Pomegranate peel enriches a variety of polyphenols such as ellagic tannins, ellagic acid and gallic acid.<sup>28</sup> Phenolics possess hydroxyl and carboxyl groups, able to interact with the zinc surface and form chelation with  $\text{Zn}^{2+}$  via chemical adsorption. Ultimately, heating and calcination of obtained powder led to the cleavage of Zn-phytochemical chelate to form nano zinc oxide.<sup>34-35</sup>

Energy-dispersive X-ray analysis (EDXA) of the synthesized nanoparticle (Figure 6) shows that the obtained PEF-ZnO NPs was composed of zinc and oxygen with no impurities which was in good agreement with the X-ray diffraction measurements.

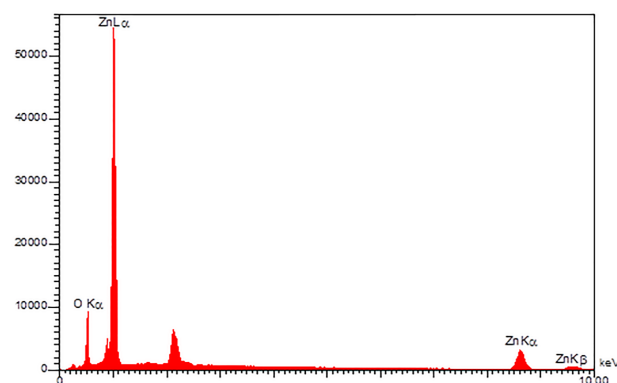


**Figure 6.** EDX analysis plot of ZnO NPs synthesized using PEF of pomegranate peel. The unlabeled peak originated from Au element used for coating samples.

**Table 1.** Antibacterial activity of ZnO nanoparticles (mg/ml).

Bacteria	Ampicillin		PEF of pomegranate peel		PEF-ZnO NPs		Commercial ZnO NPs	
	MIC	MBC	MIC	MBC	MIC	MBC	MIC	MBC
<i>S. aureus</i>	0.12	0.21	0.015	0.5	0.12	<8	0.25	<8
<i>E. coli</i>	0.24	0.41	0.031	8	0.12	<8	4	<8

### Antibacterial evaluation of ZnO NPs

Antibacterial activity of PEF of pomegranate peel, PEF-ZnO NPs and commercial ZnO NPs was determined by MIC and MBC methods against *S. aureus* and *E. coli* bacterial strains. Interestingly, PEF of pomegranate peel showed potent antibacterial inhibition against both test bacteria (<0.03 mg/ml). The growth of both bacterial strains was inhibited entirely at 0.12 mg/ml concentration of PEF-ZnO NPs. In contrast, commercial ZnO NPs prevented the growth of *S. aureus* and *E. coli* at a concentration of 0.25 and 4 mg/ml, respectively (Table 1).

The results of antibacterial activity were in accordance with previous researches that reported zinc oxide as bacteriostatic at the low concentration and bactericidal at high concentrations.<sup>24</sup> These also agreed with previous studies that reported Gram-negative bacteria is more resistant to antimicrobials that might be related to their outer membrane. Generally, the antibacterial effect of zinc oxide NPs depend on morphology, size, and concentration.<sup>34</sup> Two possible mechanisms were suggested to explain the inhibition of bacteria, namely, ROS generation on the surface of this metal oxide and interaction of zinc with the cell wall of bacteria through adhesion of ZnO NPs.<sup>36-37</sup> Liu *et al.*<sup>38</sup> published the FESEM micrographs of *E. coli* that showed the attachment of ZnO NPs on the bacterial surface. They assumed that the NPs reacted with the cell wall and damaged it, causing inhibition of the growth or death of pathogens. Ann *et al.*<sup>39</sup> also reported the same results for *S. aureus* which has exposed to ZnO NPs. However, the antibacterial properties of PEF-ZnO NPs may not entirely come from the metal ion. It may also be related to the natural antibacterial agents of the PEF of pomegranate peel remained through green synthesis. Based on literature, the biomaterial can increase the antibacterial effects of NPs.<sup>40</sup>

### Antioxidant activity

In this study, the antioxidant potential of PEF of pomegranate peel and PEF-ZnO NPs was compared with commercial ZnO NPs. DPPH assay is an in-vitro method commonly used to estimate the ability of antioxidants to neutralize free radicals. DPPH is a stable free radical that can accept an electron and reduce to its nonradical form  $\alpha, \alpha$ -diphenyl- $\beta$ -picryl hydrazine in the presence of hydrogen donors. The reduction process caused the decolorization of DPPH solution from deep purple to yellow which can be measured spectrophotometrically. The decrease of absorbance at 517 nm was calculated and detected as a capacity of DPPH scavenging activity of samples.<sup>14,41</sup> In this study, PEF of pomegranate peel showed the highest IC50 value of 9  $\mu$ g/ml, followed by gallic acid (40.31  $\mu$ g/ml)

and PEF-ZnO NPs (294.3  $\mu$ g/ml). Meanwhile, commercial ZnO NPs showed no antioxidant activity in any of the concentrations. To the depth of our knowledge, there is no report on the antioxidant activity of synthetic chemical NPs. As depicted in Figure 7 the antioxidant activity of PEF of pomegranate peel was significantly higher than that of gallic acid as a standard at all concentrations. However, PEF-ZnO NPs showed moderate antioxidant power at high concentrations. Thus the results prove that PEF-ZnO NPs would contain natural antioxidant agents through green synthesis. The antioxidant potential of green ZnO NPs has been previously reported by Stan *et al.*<sup>40</sup> Singh *et al.*<sup>30</sup> observed that different extracts of pomegranate peels and seeds have the ability to reduce the DPPH radical. Pomegranate extract is a rich source of polyphenols such as Ellagic acid and anthocyanidins which are known as powerful antioxidant agents.<sup>35</sup> These metabolites may also act as reducing agents in the synthesis process of ZnO NPs.

### In vitro SPF assessment

Figure 8 displays how the SPF values differed significantly between the samples. The emulsion containing only PEF of pomegranate peel showed SPF of 3.42, which is in good agreement with the UV-VIS spectrum ( $\lambda_{max}$ =365 nm) of this powder (Figure 2). Moreover, the high phenolic content and antioxidant power of the PEF powder could indirectly contribute to the photoprotection by capturing and inactivating reactive oxygen species. The emulsion containing commercial ZnO NPs obtained the highest SPF value (9) followed by the emulsion of green synthesized PEF-ZnO NPs (7.5). It can be attributed to the different granulometry of NPs. Fe-SEM and XRD results showed that the average size of green synthesized ZnO NPs (22

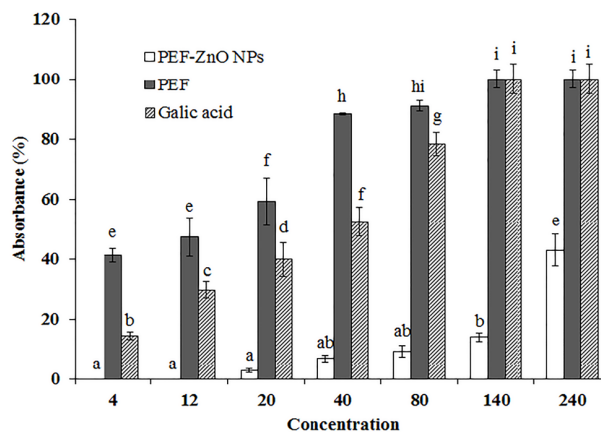


**Figure 7.** Radical scavenging activity of PEF powder and its bio-synthesized ZnO NPs in compare with Gallic acid using the DPPH method at different concentrations.

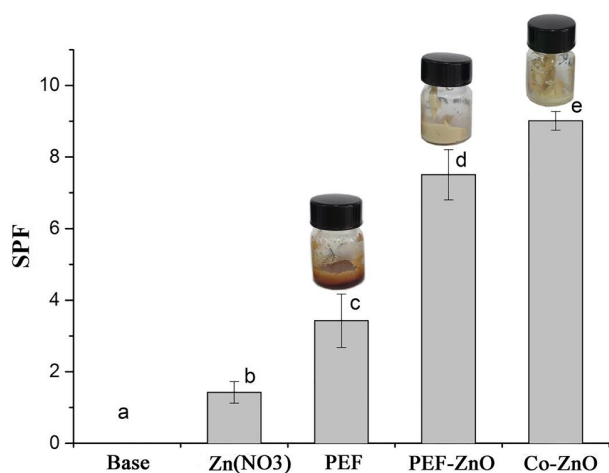


**Figure 8.** SPF values of commercial (Co.) and green synthesized (PEF) ZnO NPs in comparison with the basic emulsion and the original materials used for the synthesis.

nm) is larger than the commercial ones (17 nm). Optical properties strongly influenced by size and shape.<sup>42</sup> Thus, the photoprotection results can be attributed to the different granulometry of both NPs, especially after applying in the emulsion. Generally, the absorption curve is expected to blue-shifts with a decrease in particle size.<sup>42</sup> However, it should be noticed that UV-filters in personal care products can be effective when they remain on the surface of the skin. Generally, a decrease in particle size increases the chance of cellular uptake of the particles. Although the granulometry of PEF-ZnO NPs, in this study, resulted in less SPF value in comparison with commercial ZnO NPs, it will cause more stability on the surface of the skin leading to better protection. Furthermore, properties such as better antioxidant and antibacterial activity, along with less toxic by-products during the synthesis process, are the benefits of the prepared NPs in comparison with its chemosynthesized counterpart.

Interestingly, UV-A protection of both NPs got the same high score according to the FDA method described by Wang *et al.*<sup>19</sup> However, the ratio of green synthesized ZnO NPs was slightly higher (0.94) than commercial ZnO NPs (0.92) (Table 2). It is known that the method of synthesis determines granulometry and consequently, the optical properties of the particles.<sup>42</sup>

Due to the abundance and availability of pomegranate peel

**Table 2.** The ratio of UV-A protection in different emulsions containing commercial/green synthesized ZnO NPs and PEF of pomegranate peel.

Samples	The present study		Ratings <sup>17</sup>	
	UVA1/total UV	Ratio	Ratio	Rating
PEF powder	0.78	≥ 0.4	≥ 0.4	Low
PEF-ZnO NPs	0.94	≥ 0.4	≥ 0.4	Medium
Commercial ZnO NPs	0.92	≥ 0.7	≥ 0.7	High
		> 0.95	> 0.95	Highest

as agro-waste, mass production of polyphenol enriched fraction is practically possible. This subtle, water-soluble powder exhibited higher antibacterial and antioxidant activity than the standards (Figure 7, Table 1). So, it can provide not only a cost-effective and eco-friendly source as a precursor of green synthesis, but also can directly use in cosmeceuticals. The obtained PEF-ZnO NPs could be effectively used in the cosmetics and food industry and also can address future medical concerns. Using the PEF of pomegranate peel for the biosynthesis of other metal oxide NPs is recommended.

### Conclusion

The spherical ZnO NPs with an average diameter of 22 nm were successfully biosynthesized using a polyphenol enriched fraction of pomegranate peel. The morphology, purity, and quality of biosynthesized PEF-ZnO NPs were highly comparable with its commercial counterpart and it also exhibited good antibacterial and antioxidant activity. Moreover, evaluation of sunscreen potential of PEF-ZnO NPs in water-in-oil emulsions showed SPF and UV-A values of 7.5 and 0.94, respectively. These results open the possibility to apply pomegranate waste materials in sunscreen productions and design a safe alternative to harmful chemical precursors currently used for the synthesis of metal oxide NPs.

### Conflict of Interest

The authors claim that there is no conflict of interest.

### References

- Volpe A, Pagano M, Mascolo G, Grenni P, Rossetti S. Biodegradation of UV-filters in marine sediments. *Sci Total Environ.* 2017;575:448-57. doi:10.1016/j.scitotenv.2016.10.001
- Ganesan P, Choi DK. Current application of phytocompound-based nanocosmeceuticals for beauty and skin therapy. *Int J Nanomedicine.* 2016;11:1987-2007. doi:10.2147/IJN.S104701
- Shashanka R, Kamacı Y, Taş R, Ceylan Y, Savaş Bülbül A, Uzun O, et al. Antimicrobial investigation of CuO and ZnO nanoparticles prepared by a rapid combustion method. *Phys Chem Res.* 2019;7(4):799-812. doi:10.22036/pcr.2019.199338.1669
- Aminuzzaman M, Ying LP, Goh W-S, Watanabe A. Green synthesis of zinc oxide nanoparticles using aqueous extract of *Garcinia mangostana* fruit pericarp and their photocatalytic activity. *Bull Mater Sci.* 2018;41:50. doi:10.1007/s12034-018-1568-4
- Shashanka R. Synthesis of silver nanoparticles and their applications. *Anal Bioanal Electrochem.* 2013;5(4):455-66.
- Shashanka R, Cahit Karaoglanli A, Ceylan Y, Uzun O. A fast and robust approach for the green synthesis of spherical magnetite (Fe<sub>3</sub>O<sub>4</sub>) nanoparticles by *Tilia tomentosa* (ihlamur) leaves and its antibacterial studies. *Pharm Sci.* 2020;26(2):175-83. doi:10.34172/ps.2020.5

7. Kathiresan K, Manivannan S, Nabeel MA, Dhivya B. Studies on silver nanoparticles synthesized by a marine fungus, *Penicillium fellutanum* isolated from coastal mangrove sediment. *Colloid Surface B*. 2009;71(1):133-7. doi:10.1016/j.colsurfb.2009.01.016
8. Doan VD, Luc VS, Nguyen TL, Nguyen TD, Nguyen TD. Utilizing waste corn-cob in biosynthesis of noble metallic nanoparticles for antibacterial effect and catalytic degradation of contaminants. *Environ Sci Pollut Res*. 2019;27:6148-62. doi:10.1007/s11356-019-07320-2
9. Tehranifar A, Zarei M, Nemati Z, Esfandiari B, Vazifeshenas MR. Investigation of physico-chemical properties and antioxidant activity of twenty Iranian pomegranates (*Punica granatum* L.) cultivars. *Sci Hortic* 2010;126(2):180-5. doi:10.1016/j.scienta.2010.07.001
10. Akhtar S, Ismail T, Fraternali D, Sestili P. Pomegranate peel and peel extracts: Chemistry and food features. *Food Chem*. 2015;174:417-25. doi:10.1016/j.foodchem.2014.11.035
11. Mishra T, Pal M, Kumar A, Rai D, Tewari SK. Termiticidal activity of *punica granatum* fruit rind fractions and its compounds against *Microcerotermes besoni*. *Ind Crop Prod*. 2017;107:320-5. doi:10.1016/j.indcrop.2017.05.030
12. Patterson A. The scherrer formula for x-ray particle size determination. *Phys Rev*. 1939;56:978-82. doi:10.1103/PhysRev.56.978
13. Rajabi HR, Naghiha R, Kheirizadeh M, Sadatfaraji H, Mirzaei A, Alvand ZM. Microwave assisted extraction as an efficient approach for biosynthesis of zinc oxide nanoparticles: Synthesis, characterization, and biological properties. *Mater Sci Eng C*. 2017;78:1109-18. doi:10.1016/j.msec.2017.03.090
14. Luo X, Cui J, Zhang H, Duan Y, Zhang D, Cai M, et al. Ultrasound assisted extraction of polyphenolic compounds from red sorghum (*Sorghum bicolor* L.) bran and their biological activities and polyphenolic compositions. *Ind Crop Prod*. 2018;112:296-304. doi:10.1016/j.indcrop.2017.12.019
15. Kokabi M, Yousefzadi M, Soltani M, Arman M. Effects of different UV radiation on photoprotective pigments and antioxidant activity of the hot-spring cyanobacterium *Leptolyngbya cf. fragilis*. *Phycol Res*. 2019;67(3):215-20. doi:10.1111/pre.12374
16. Maske PP, Lokapure SG, Nimbalkar D, Malavi S, D'Souza JI. *In vitro* determination of sun protection factor and chemical stability of *Rosa kordesii* extract gel. *J Pharm Res*. 2013;7(6):520-4. doi:10.1016/j.jopr.2013.05.021
17. Bendova H, Akrman J, Krejci A, Kubac L, Jirova D, Kejlova K, et al. *In vitro* approaches to evaluation of sun protection factor. *Toxicol In Vitro*. 2007;21(7):1268-75. doi:10.1016/j.tiv.2007.08.022
18. Reis Mansur MCPP, Leitão SG, Cerqueira-Coutinho C, Vermelho AB, Silva RS, Presgrave OAF, et al. *In vitro* and *in vivo* evaluation of efficacy and safety of photoprotective formulations containing antioxidant extracts. *Rev Bras Farmacogn*. 2016;26(2):251-8. doi:10.1016/j.bjp.2015.11.006
19. Wang SQ, Stanfield JW, Osterwalder U. *In vitro* assessments of uva protection by popular sunscreens available in the united states. *J Am Acad Dermatol*. 2008;59(6):934-42. doi:10.1016/j.jaad.2008.07.043
20. Moghadam SE, Ebrahimi SN, Gafner F, Ochola JB, Marubu RM, Lwande W, et al. Metabolite profiling for caffeic acid oligomers in *Satureja biflora*. *Ind Crops Prod*. 2015;76:892-9. doi:10.1016/j.indcrop.2015.07.059
21. Seeram N, Lee R, Hardy M, Heber D. Rapid large scale purification of ellagitannins from pomegranate husk, a by-product of the commercial juice industry. *Separation and purification technology*. 2005 1;41(1):49-55. doi:10.1016/j.seppur.2004.04.003
22. Talam S, Karumuri SR, Gunnam N. Synthesis, characterization, and spectroscopic properties of ZnO nanoparticles. *ISRN Nanotechnology*. 2012;372505. doi:10.5402/2012/372505
23. Elumalai K, Velmurugan S. Green synthesis, characterization and antimicrobial activities of zinc oxide nanoparticles from the leaf extract of *Azadirachta indica* (L.). *Appl Surf Sci*. 2015;345:329-36. doi:10.1016/j.apsusc.2015.03.176
24. Ali K, Dwivedi S, Azam A, Saquib Q, Al-Said MS, Alkhedhairy AA, et al. *Aloe vera* extract functionalized zinc oxide nanoparticles as nanoantibiotics against multi-drug resistant clinical bacterial isolates. *J Colloid Interface Sci*. 2016;472:145-56. doi:10.1016/j.jcis.2016.03.021
25. Singh J, Kumar S, Alok A, Upadhyay SK, Rawat M, Tsang DCW, et al. The potential of green synthesized zinc oxide nanoparticles as nutrient source for plant growth. *J Clean Prod*. 2019;214:1061-70. doi:10.1016/j.jclepro.2019.01.018
26. Hong RY, Li JH, Chen LL, Liu DQ, Li HZ, Zheng Y, et al. Synthesis, surface modification and photocatalytic property of ZnO nanoparticles. *Powder Technol*. 2009;189(3):426-32. doi:10.1016/j.powtec.2008.07.004
27. Rajiv P, Rajeshwari S, Venkatesh R. Bio-fabrication of zinc oxide nanoparticles using leaf extract of *Parthenium hysterophorus* L. and its size-dependent antifungal activity against plant fungal pathogens. *Spectrochim Acta A*. 2013;112:384-7. doi:10.1016/j.saa.2013.04.072
28. Edison TJ, Sethuraman MG. Biogenic robust synthesis of silver nanoparticles using *Punica granatum* peel and its application as a green catalyst for the reduction of an anthropogenic pollutant 4-nitrophenol. *Spectrochim Acta A Mol Biomol Spectrosc*. 2013;104:262-4. doi:10.1016/j.saa.2012.11.084
29. Oliveira RN, Mancini MC, Oliveira FCSD, Passos TM, Quilty B, Thiré RMDSM, et al. FTIR analysis and quantification of phenols and flavonoids of five commercially available plants extracts used in wound healing. *Rev Matéria*. 2016;21(3):767-79. doi:10.1590/

- S1517-707620160003.0072
30. Singh RP, Chidambara Murthy KN, Jayaprakasha GK. Studies on the antioxidant activity of pomegranate (*Punica granatum*) peel and seed extracts using in vitro models. *J Agric Food Chem*. 2002;50:81-6. doi:10.1021/jf010865b
  31. Sharma RK, Ghose R. Synthesis of zinc oxide nanoparticles by homogeneous precipitation method and its application in antifungal activity against *Candida albicans*. *Ceram Int*. 2015;41(1):967-75. doi:10.1016/j.ceramint.2014.09.016
  32. Santhoshkumar J, Kumar SV, Rajeshkumar S. Synthesis of zinc oxide nanoparticles using plant leaf extract against urinary tract infection pathogen. *Resource-Efficient Technologies*. 2017;3(4):459-65. doi:10.1016/j.refit.2017.05.001
  33. Ling D, Hackett MJ, Hyeon T. Surface ligands in synthesis, modification, assembly and biomedical applications of nanoparticles. *Nano Today*. 2014;9(4):457-77. doi:10.1016/j.nantod.2014.06.005
  34. Pandimurugan R, Thambidurai S. Novel seaweed capped ZnO nanoparticles for effective dye photodegradation and antibacterial activity. *Adv Powder Technol*. 2016;27(4):1062-72. doi:10.1016/j.apt.2016.03.014
  35. Ahmad N, Sharma S, Rai R. Rapid green synthesis of silver and gold nanoparticles using peels of *Punica granatum*. *Adv Mater Lett*. 2012;3(5):376-80. doi:10.5185/amlett.2012.5357
  36. Suresh J, Pradheesh G, Alexramani V, Sundrarajan M, Hong SI. Green synthesis and characterization of zinc oxide nanoparticle using insulin plant (*Costus pictus* d. Don) and investigation of its antimicrobial as well as anticancer activities. *Adv Nat Sci-Nanosci*. 2018;9(1):015008. doi:10.1088/2043-6254/aaa6f1
  37. Mirzaei H, Darroudi M. Zinc oxide nanoparticles: Biological synthesis and biomedical applications. *Ceram Int*. 2017;43(1):907-14. doi:10.1016/j.ceramint.2016.10.051
  38. Liu Y, He L, Mustapha A, Li H, Hu ZQ, Lin M. Antibacterial activities of zinc oxide nanoparticles against *Escherichia coli* O157:H7. *J Appl Microbiol*. 2009;107(4):1193-201. doi:10.1111/j.1365-2672.2009.04303.x
  39. Ann LC, Mahmud S, Bakhori SKM, Sirelkhatim A, Mohamad D, Hasan H, et al. Antibacterial responses of zinc oxide structures against *Staphylococcus aureus*, *pseudomonas aeruginosa* and *Streptococcus pyogenes*. *Ceram Int*. 2014;40(2):2993-3001. doi:10.1016/j.ceramint.2013.10.008
  40. Stan M, Popa A, Toloman D, Silipas TD, Vodnar DC. Antibacterial and antioxidant activities of ZnO nanoparticles synthesized using extracts of *Allium sativum*, *rosmarinus officinalis* and *Ocimum basilicum*. *Acta Metall Sin-Engl*. 2016;29(3):228-36. doi:10.1007/s40195-016-0380-7
  41. Kedare SB, Singh RP. Genesis and development of DPPH method of antioxidant assay. *J Food Sci Technol*. 2011;48(4):412-22. doi:10.1007/s13197-011-0251-1
  42. Truffault L, Winton B, Choquenot B, Andrezza C, Simmonard C, Devers T, et al. Cerium oxide based particles as possible alternative to ZnO in sunscreens: Effect of the synthesis method on the photoprotection results. *Mater Lett*. 2012;68:357-60. doi:10.1016/j.matlet.2011.10.108